Environment International 158 (2022) 106889

Contents lists available at ScienceDirect

Environment International

journal homepage: www.elsevier.com/locate/envint

Transcriptomic evidences for microbial carbon and nitrogen cycles in the deoxygenated seawaters of Bohai Sea

Yu Han [a], Mu Zhang [a], Xiaofeng Chen [a], Weidong Zhai [b], Ehui Tan [c], Kai Tang [a,*]

[a] State Key Laboratory of Marine Environmental Science, Fujian Key Laboratory of Marine Carbon Sequestration, College of Ocean and Earth Sciences, Xiamen University, Xiamen 361102, Fujian, PR China
[b] Institute of Marine Science and Technology, Shandong University, Qingdao 266000, Shandong, PR China
[c] State Key Laboratory of Marine Resource Utilization in South China Sea, Hainan University, Haikou 570228, Hainan, PR China

ARTICLE INFO

Handling Editor: Adrian Covaci

Keywords:
Microbial community
Oxygen
Ammonia oxidation
Metatranscriptomics
Ocean

ABSTRACT

Eutrophication-induced water deoxygenation occurs continually in coastal oceans, and alters community structure, metabolic processes, and the energy shunt, resulting in a major threat to the ecological environment. Seasonal deoxygenation events have occurred in the Bohai Sea (China), however, how these affect the functional activity of microorganisms remains unclear. Here, through the use of absolute quantification of 16S rRNA genes amplicon sequencing and metatranscriptomics approaches, we investigated the structure of the microbial community and the patterns of transcriptional activity in deoxygenated seawaters. The dominant phyla were Proteobacteria (average value, 1.4×10^6 copies ml^{-1}), Cyanobacteria (3.7×10^5 copies ml^{-1}), Bacteroidetes (2.7×10^5 copies ml^{-1}), and the ammonia-oxidizing archaea Thaumarchaeota (1.9×10^5 copies ml^{-1}). Among the various environmental factors, dissolved oxygen, pH and temperature displayed the most significant correlation with microbial community composition and functional activity. Metatranscriptomic data showed high transcriptional activity of Thaumarchaeota in the deoxygenated waters, with a significant increase in the expression of core genes representing ammonia oxidation, ammonia transport, and carbon fixation (3-hydroxypropionic acid/4-hydroxybutyric acid cycle) pathways. The transcripts of Cyanobacteria involved in photosynthesis and carbon fixation (Calvin-Benson-Bassham cycle) significantly decreased in low oxygen waters. Meanwhile, the transcripts for the ribulose bisphosphate carboxylase-encoding gene shifted from being assigned to photoautotrophic to chemoautotrophic organisms in surface and bottom waters, respectively. Moreover, the transcription profile indicated that heterotrophs play a critical role in transforming low-molecular-weight dissolved organic nitrogen. Elevated abundances of transcripts related to microbial antioxidant activity corresponded to an enhanced aerobic metabolism of Thaumarchaeota in the low oxygen seawater. In general, our transcriptional evidences showed a population increase of Thaumarchaeota, especially the coastal ecotype of ammonia oxidizers, in low oxygen aquatic environments, and indicated an enhanced contribution of chemolithoautotrophic carbon fixation to carbon flow.

1. Introduction

Dissolved oxygen (DO) levels in the oceans have been persistently falling over the past 50 years, and the global ocean is expected to lose approximately 3–4% of oxygen capacity by the end of this century (Keeling et al., 2010; Laffoley and Baxter, 2019; Schmidtko et al., 2017). Subsequently, hypoxia (DO concentration $\leq$2 mg l^{-1}) has inevitably occurred in some areas (Breitburg et al., 2018). DO reduction will directly threaten the growth and survival of aerobic organisms in aquatic ecosystems, increasing the pressure on ecosystem sustainability, reducing biodiversity and the yield of fisheries (Breitburg et al., 2018). The decline of DO will also constrain ecosystem energetics, alter the ecosystem structure, and drastically affect microbial-mediated biogeochemical cycling of elements such as carbon, nitrogen, phosphorus, and trace metals (Vaquer-Sunyer and Duarte, 2008; Wright et al., 2012). The microbial diversity of community composition and metabolic processes can be dramatically affected by hypoxia, for example, nitrate reduction and sulfur oxidation processes can be stimulated in low oxygen waters

* Corresponding author at: State Key Laboratory of Marine Environmental Science, Fujian Key Laboratory of Marine Carbon Sequestration, College of Ocean and Earth Sciences, Xiamen University, Xiamen 361102, PR China.
E-mail address: tangkai@xmu.edu.cn (K. Tang).

https://doi.org/10.1016/j.envint.2021.106889
Received 26 December 2020; Received in revised form 19 September 2021; Accepted 20 September 2021
Available online 4 October 2021

(Ulloa et al., 2012; Wright et al., 2012). Climate warming, as one of the known ocean deoxygenation mechanisms, directly decreases oxygen solubility, slows down water circulation via intensified stratification, and also promotes microbial respiration, resulting in a decrease of DO concentration (Oschlies et al., 2018). Excessive nutrient discharge-induced eutrophication in coastal waters is another important driver for the frequent occurrence of hypoxia. Sustained nutrient input will stimulate primary productivity in the euphotic zone. Increased productivity will then generate more organic matter to fuel heterotrophs, and promote microbial respiration in both the water column and sediments (Cai et al., 2019; Laffoley and Baxter, 2019; Robinson, 2019), consuming a large amount of DO, leading to coastal ecosystems facing more serious deoxygenation environmental problems (Robinson, 2019; Zhang et al., 2010). Statistics indicate that since the 1950s, more than 900 coastal areas around the world are facing eutrophication problems, of which more than 700 have been experiencing hypoxia or anoxia (Breitburg et al., 2018; Laffoley and Baxter, 2019). Unfortunately, ocean deoxygenation will continually occur in the future due to the persistent climate change and anthropogenic activities (Laffoley and Baxter, 2019).

Microorganisms, including bacteria and archaea, while small in size, are highly abundant with an extremely large collective biomass, and the main conduits of material and energy flow in marine ecosystems (Karl, 2002). Ocean deoxygenation will force ecosystem material and energy flows to shift from higher-level predations toward lower-level microorganisms (Jessen et al., 2017; Wright et al., 2012). Studies have indicated that microorganisms can still grow aerobically in low oxygen environments and even under hypoxia condition (Kalvelage et al., 2015). Most of the studies on hypoxic zones have mainly focused on the formation mechanisms of hypoxia and their impacts on the biogeochemical cycles of biogenic elements, such as carbon, nitrogen, and sulfur (Fennel and Testa, 2019; Zhai et al., 2019). However, the adaptive mechanisms and environmental regulating factors for microorganisms in deoxygenated waters have rarely been investigated. The functional activities, particularly their roles in mediating carbon and nitrogen cycles in low oxygen waters, are still unclear.

High-throughput 16S rRNA sequencing, quantitative real-time PCR (qPCR), and meta-omics methods have generally been applied to study the microbial community and their related functions (Spietz et al., 2015; Walters et al., 2015; Ye et al., 2016). Of these methods, the use of high-throughput 16S rRNA sequencing for detection of archaea is limited due to primer design (Walters et al., 2015), while qPCR is usually applied in the quantitative analysis of functional genes (Gillies et al., 2015). In addition to these two methods, metatranscriptome has the advantages of characterizing the expressed functions of the total microbial community (Hewson et al., 2013; Stewart et al., 2012). However, microbial metatranscriptome related studies are still relatively rare in costal deoxygenated environments, relative to the high-throughput 16S rRNA sequencing and/or qPCR (Gillies et al., 2015; Hewson et al., 2013; Lekunberri et al., 2013; Molina et al., 2010).

Recently, the typical coastal areas of China, including the Yangtze River Estuary, Pearl River Estuary, Yellow Sea, and Bohai Sea, have experienced seasonal deoxygenation events, with low oxygen or hypoxia zones generally observed from June to September (Chen et al., 2007; Qian et al., 2018; Zhai et al., 2019). Here, seawater with a DO concentration between the conventional definition of hypoxia and the oxygen-saturation condition is considered to be “low oxygen seawater”. Using high-throughput 16S rRNA sequencing and metatranscriptomics, we investigated the dynamics of community composition and transcriptional activity of the dominant bacteria and archaea in the deoxygenated Bohai Sea. We thus compared the dominant prokaryotic groups and their functional activities in low oxygen seawater with those in oxygen-saturation environments to reveal the microbial-mediated carbon and nitrogen cycles in deoxygenated environments at the transcriptomic level.

2. Experimental procedures

2.1. Sampling and pretreatment

Samples were collected from two sites (A31: 39.28°N, 119.56°E; A45: 39.20 °N, 119.78°E) in the Bohai Sea, China, during a cruise conducted on August 28–30, 2018 (Fig. 1). Seawater samples were collected using 10 L Niskin bottles attached to a conductivity-temperature-depth (CTD) rosette sampler from three depths, the surface, middle, and bottom layers (see specific depth values in Table 1), depending on the total water depth and thermocline at each station. The DO concentration was instantaneously measured on board using the Winkler method. In this paper, low oxygen seawater was defined between hypoxia ($\leq$2 mg l^{-1}) to the oxygen-saturation condition ($\geq$7 mg l^{-1}, according to the field measured data) of DO (Hewson et al., 2013; Keeling et al., 2010; Vaquer-Sunyer and Duarte, 2008). The low oxygen region was then identified according to the distribution of DO concentration in both surface and bottom water (Fig. 1). Sites A31 and A45 were characterized by similar hydrological conditions but different DO concentrations (Fig. 1b and Table 1). The DO concentrations ranged from 5.11 to 5.47 mg l^{-1} and from 3.92 to 3.96 mg l^{-1} below the surface layer of sites A31 and A45, respectively, representing low oxygen environments; while the surface was saturated in oxygen (Fig. 1a and Table 1). Therefore, samples from surface and non-surface layers were chosen for a comparison. The samples for 16S rRNA genes and metatranscriptomes analyses were obtained from two discrete size fractions, 0.2–3.0 μm and 3.0–20 μm, representing the free-living and particle-associated states, respectively (Teeling et al., 2012). The corresponding size-fractionated biomass was collected by sequential inline filtration of seawater orderly through a nylon screen (200 μm, LABLEAD.Inc), a polycarbonate filter (47 mm, 3.0 μm pore size, Millipore, USA), and a second polycarbonate filter (47 mm, 0.22 μm pore size, Millipore, USA). Samples for metatranscriptomic analysis were obtained in duplicate and preserved in RNAlater (Applied Biosystems, Austin, TX) for further treatment. In addition, dissolved organic carbon (DOC) samples in triplicate were directly collected and preserved at 4 °C after addition of H_3PO_4. Dissolved inorganic carbon (DIC) samples were collected using 60 ml borosilicate glass bottles, then sealed with screw-on caps and stored at room temperature after addition of 50 μl saturated $HgCl_2$. About 500 ml of seawater was filtered through a precombusted (450 °C for 4 h) GF/F membrane (Whatman, 47 mm diameter) to collect filtrate and suspended particulate matter. The filtrate was stored at −20 °C for later nitrate (NO_3-N), nitrite (NO_2-N), ammonium (NH_4-N), dissolved inorganic phosphate (DIP), and dissolved silicate (DSi) concentration analysis. The filters were stored at −20 °C until the measurement of Chlorophyll *a* (Chl *a*), particulate organic carbon (POC) and organic nitrogen (PON) contents in the laboratory.

2.2. Environmental measurements

Seawater temperature, pH, and salinity were measured with CTD probes (OCEAN SEVEN 304 Plus, Italy). DO was measured on board using the Winkler method. The DO saturation (DO%) was calculated as the field-measured DO concentration divided by the DO concentration at equilibrium with the atmosphere (Benson and Krause, 1984). After returning to the laboratory, DIC analyses, based on the methods described in Cai et al. (2004) with a precision of ±2 μmol kg^{-1}, were performed. Chl *a* concentration was measured using high performance liquid chromatography as described in Zapata et al. (2000). The concentrations of NO_3-N, NO_2-N, DIP, and DSi were analyzed according to standard colorimetric methods with a Technicon AA3 Auto-Analyzer (Bran-Luebbe) (Dai et al., 2008). The NH_4-N concentration was measured on the deck using the indophenol blue spectrophotometric method (Pai et al., 2001). DOC concentration was quantified using high-temperature catalytic combustion with a Shimadzu TOC-VCPH/CPN Total Organic Carbon Analyzer equipped with an ASI-V autosampler

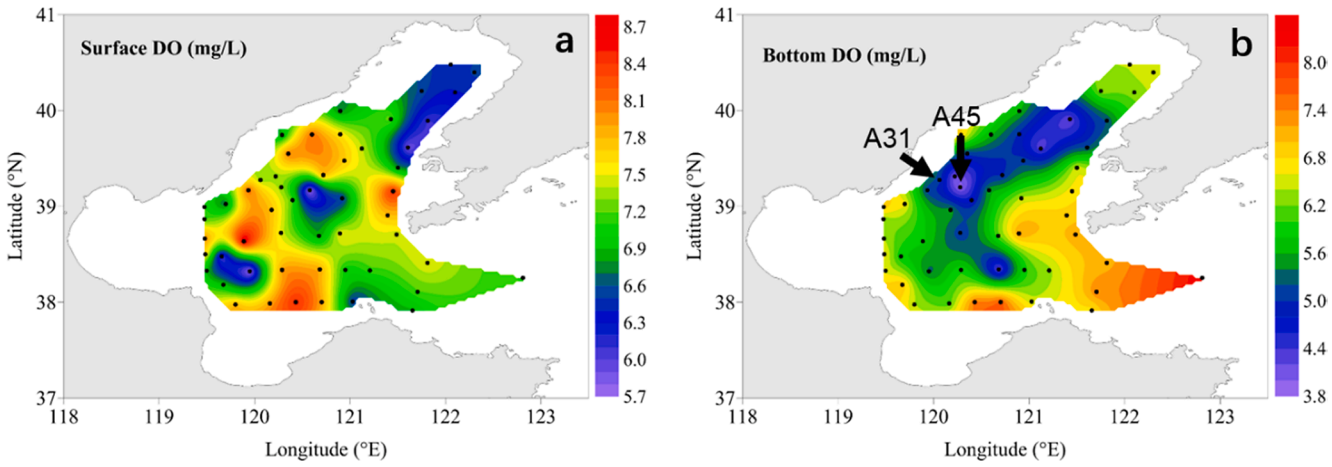

Fig. 1. Sampling sites and survey-based distribution of dissolved oxygen in (a) surface and (b) bottom water. The lowest DO concentrations in bottom water were observed at sites A45 and A31.

Table 1
Environmental parameters at two deoxygenated sites (A31 and A45) in the Bohai Sea. Abbreviations: DO, Dissolved oxygen; Chl *a*, Chlorophyll *a*; DIC: Dissolved inorganic carbon; DIP: Dissolved inorganic phosphate; DSi: Dissolved silicate; DOC, Dissolved organic carbon; POC: Particle organic carbon; PON, Particle organic nitrogen; TPA: Total prokaryotic abundance.

Factors	A31			A45		
	Surface	Middle	Bottom	Surface	Middle	Bottom
Depth (m)	4	11	20	3	13	24
DO (mg l^{-1})	7.33	5.47	5.11	7.34	3.96	3.92
DO (%)	106.90	77.30	71.90	105.90	55.50	54.90
pH_T	8.01	7.88	7.85	8.02	7.75	7.76
Temperature (°C)	25.71	23.91	23.69	25.32	23.53	23.52
Salinity (‰)	30.76	30.77	30.78	30.83	30.88	30.88
Chl *a* (ng l^{-1})	424.64	718.41	356.42	368.95	207.45	165.68
DIC (μmol kg^{-1})	2154.84	2234.74	2256.07	2173.65	2289.97	2291.59
NO_3-N (μmol l^{-1})	0.51	3.88	5.40	0.12	9.41	9.44
NO_2-N (μmol l^{-1})	0.13	0.39	0.51	0.09	0.34	0.36
NH_4-N (μmol l^{-1})	0.46	0.40	0.34	0.41	0.14	0.22
DIP (μmol l^{-1})	0.03	0.12	0.17	0.09	0.48	0.49
DSi (μmol l^{-1})	3.47	9.84	11.51	9.49	18.85	22.16
DOC (μmol l^{-1})	179.70 ± 2.64	150.61 ± 14.36	152.79 ± 8.06	209.93 ± 15.10	168.54 ± 33.10	147.48 ± 2.22
POC (μg l^{-1})	216.21 ± 3.29	170.82 ± 7.35	221.47 ± 20.02	284.87 ± 6.17	143.56 ± 15.59	162.56 ± 2.52
PON (μg l^{-1})	33.34 ± 0.25	26.40 ± 0.31	30.18 ± 1.50	52.02 ± 1.39	22.43 ± 0.55	21.74 ± 0.95
TPA (10^6 cell ml^{-1})	7.66 ± 0.38	4.51 ± 0.30	4.62 ± 0.21	5.47 ± 0.25	3.23 ± 0.18	3.21 ± 0.79

and a TNM-1 module (Osterholz et al., 2014). Filters were freeze dried and then acidified with 1 ml of 1 N HCl solution to remove carbonate. All filters were dried again at 60 °C in an oven for 48 h. The POC and PON contents of the decarbonated samples were determined with an Elemental Analyzer (Carlo-Erba EA 2100; Kao et al., 2012). Total prokaryotic abundance was measured by a Accuri C6 flow cytometer (BD Biosciences) after the cells were stained with SYBR Green I (Dominique et al., 1997).

2.3. The relative and absolute quantification of 16S rRNA genes

Microbial community genomic DNA was extracted using the PowerSoil DNA Isolation Kit (MoBio, Carlsbad, USA). The description for the absolute quantification of 16S ribosomal RNA (rRNA) genes has been previously outlined in Tkacz et al. (2018). Briefly, two or three spike-in sequences at four different concentrations (10^3, 10^4, 10^5, 10^6 copies of internal standards) were added to the sample DNA pools. The spike-in sequences contained conserved regions identical to those of natural 16S rRNA genes and artificial variable regions different from nucleotide sequences in the public databases, acting as an internal standard and allowing absolute quantification and comparison across samples (Jiang et al., 2019). The V4 region of the archaeal and bacterial 16S rRNA genes was amplified with modified primer pairs 515F mod (5′-GTGYCAGCMGCCGCGGTAA-3′) and 806R mod (5′-GGACTACNVGGGTWTCTAAT-3′) (Walters et al., 2015) and then sequenced on an Illumina MiSeq.

2.4. Illumina read data processing

The raw sequencing data was processed as previously described in Huang et al. (2015). The adaptor and primer sequences were removed by using TrimGalore and Mothur, respectively. After pair-end reads were merged and filtered, low quality reads (<200 bp, average quality score < 20, ambiguous base calls > 0) were discarded. Operational taxonomic units (OTUs) with 97% similarity cutoff were clustered using USEARCH (version 10). Taxonomic annotation was performed at a confidence threshold of 80% by Mothur (version 1.41.1) with the command classify.seqs based on the RDP (version 11.5) database. The absolute copies of prokaryotic OTUs were subsequently calculated via a standard curve established by read-counts versus spike-in OTUs copies. Amplicon sequence variants (ASVs) was sufficiently achieved by DADA2 plug-in QIIME 2 (Bolyen et al., 2019; Callahan et al., 2017). Taxonomy was assigned to the ASVs against in SILVA 138 100% OTUs using q2-feature-classifier's classify-sklearn method with a confidence of 80

(Bolyen et al., 2019; Bokulich et al., 2018). Similarly, the quantification of ASVs was conducted by applying the abovementioned method. The raw reads from this study were deposited into the NCBI Sequence Read Archive (SRA) under accession numbers SRR11179217- SRR11179228.

2.5. Metatranscriptomics

Gene-expression patterns of microbial communities were assessed by metatranscriptomic analysis. Total RNA was extracted using the MoBio PowerSoil Total RNA Isolation Kit (MO BIO Laboratories, Inc.) following the manufacturer's instructions. The extraction was digested with 5U DNaseI (Takara, Japan) at 37 °C for 30 min. RNA was purified using a RNeasy MinElute Cleanup Kit (Qiagen, Germany), followed by treatment with an Ribo-Zero™ Magnetic Kit (Epicentre, USA) to remove rRNA. Sequencing libraries made from the rRNA-depleted samples were constructed with a NEB Next® Ultra™ Directional RNA Library Prep Kit for Illumina (NEB, USA). The remaining transcripts were linearly amplified, and converted to double stranded complementary DNA (cDNA) for library preparation and sequencing. rRNA-depleted samples were processed using the First Strand short Reaction Buffer (5X) with Random Primers to split mRNA, and mRNA was converted into cDNA using the Murine RNase Inhibitor, Actinomycin D, and the ProtoScript II Reverse Transcriptase, followed by Second Strand Synthesis Buffer with dUTP Mix (10X) and the Second Strand Synthesis Enzyme Mix. After purification with AMPure XP Beads (Agencourt, USA), terminal repair and connection was performed using the End Repair Reaction Buffer (10X) and the End Prep Enzyme Mix, followed by the NEBNext Adaptor and the Blunt/TA Ligase Master Mix. Synthesized cDNA was purified using AMPure XP Beads, and amplified using USER Enzyme with Universal PCR Primer and Index (X) Primer. Subsequent purification was performed with AMPure XP Beads to obtain libraries for sequencing. The cDNA was detected using the TruSeq PE Cluster Kit (Illumina, USA) in cBot to generate clusters, and libraries were sequenced on the Illumina HiSeq 4000 platform to obtain paired-end reads. A total of 2.2 billion sequence reads with a mean length of 150 bp were obtained from 33 samples (Table S1). One sample (A31_B_PA) had insufficient total RNA level and was therefore not included in further analyses (Table S2). The raw reads from this study were deposited into the NCBI Sequence Read Archive (SRA) under accession numbers SRR10800987-SRR10801019.

2.6. Bioinformatic processing

rRNA sequences were identified and removed according to the reads comparison among NCBI (rRNA and tRNA) and SILVA (www.arb-silva.de) databases. The remaining mRNA sequences were assembled from scratch using the Trinity software. Sequences from all samples were then integrated and CD-Hit-Est was applied to remove redundancy (the sequence consistency threshold was set at 0.95). Gene prediction was applied based on the splicing Scaffold (Schulz et al., 2012), and subsequently microbial gene sequences were functionally annotated. Gene transcript abundance was calculated by counting the number of reads that were aligned by Samtools (Li et al., 2009), and normalized to the gene length. Transcripts were queried against the NCBI non-redundant protein sequence database (http://ncbi.nlm.nih.gov/), Kyoto Encyclopedia of Genes and Genomes database (http://www.kegg.jp) (Kanehisa and Goto, 2000), evolutionary genealogy of genes: Non-supervised Orthologous Groups database (http://eggnogdb.embl.de/) (Huerta-Cepas et al., 2016), Uniprot database (http://www.uniprot.org/) (UniProt, 2015), and the SEED database (http://www.theseed.org/wiki/Main_Page) to identify a probable function (Overbeek et al., 2005). DIAMOND was used to perform blastp homology comparison between gene set protein sequences and the databases mentioned above to obtain functional annotation and homologous species information (Screening criteria: e-value < 1e−5, score > 60) (Huson and Buchfink, 2015). At the same time, according to the NCBI microbiological taxonomy information database, the species classification annotation information of genes was obtained, and the relative abundance of species was counted at multiple taxonomic levels. The amino acid sequences were submitted to CAZyme Annotation Toolkit (http://mothra.ornl.gov/cgibin/cat/cat.cgi) for sequence-based annotation (e-value < 1e−5, score > 60) (Lombard et al., 2013; Park et al., 2010). The manually selected sequences of dissolved organic nitrogen (DON) membrane transporters were blasted (e-value < 1e−5) against the Transporter Classification Database (http://www.tcdb.org) (Saier et al., 2009). The results were then further checked manually. For the expression of DON transporter- and antioxidant enzyme-encoding genes, the transcripts were normalized to the corresponding phyla of absolute quantitative copy counts to reveal the transcriptional activity of a single cell. The significance of transcript variation was calculated and statistically examined by Student's *t*-test analysis using GraphPad Prism 8.0.2 (GraphPad Software, USA).

2.7. Statistical analysis

The spatial variation of environmental factors was statistically examined by one-way analysis of variance (ANOVA). Student's *t*-tests were conducted to examine the difference in microbial community at a confidence of 95% using GraphPad Prism 8.0.2 (GraphPad Software, USA). Before the correlation analysis between microbial community composition and environmental factors, Mantel test was performed to determine statistically significant correlation via PAleontological Statistics (PAST, Version 3.25). Bray-Curtis and Euclidean were selected to calculate similarity index for OTUs and for environmental parameters with 9,999 permutations during Mantel test, respectively. The correlations between environmental factors and dominant microbial groups were achieved using Spearman's correlation analysis. All statistical analyses with p value < 0.05 were significant. Specific p values ($p < 0.05$, 0.01, 0.001, 0.0001) are marked at the corresponding places. According to the relative and absolute 16S OTUs analysis and metatranscriptome sequence analysis, the top 10 identified cultured groups were defined as abundant groups, while the remaining groups were regarded as less abundant groups.

3. Results

3.1. Environmental conditions

The environmental parameters from the three sampling depths of two sites are shown in Table 1. The DO concentration was slightly oversaturated in the surface water and then decreased with depth to a value of 5.11 mg l^{-1} and 3.92 mg l^{-1} in bottom water at sites A31 and A45, respectively (Fig. 1 and Table 1). Site A45 was the center of a low oxygen zone during the sampling period (Fig. 1b). Both pH and temperature presented a decreasing trend with depth, while the salinity was relatively stable with a value of ~31 regardless of sampling depth, representing similar hydrological conditions at the two study sites (Table 1). The Chl *a* concentration at site A31 varied from 356.4 to 424.6 ng l^{-1}, and was relatively higher than that at site A45 (with a range of 165.7–368.9 ng l^{-1}, Table 1). The distribution pattern of DIC concentration at the two sites was similar with a slight increase from surface to bottom water (Table 1). The concentrations of NO_3-N, NO_2-N, DIP, and DSi, all increased with increasing depth, of which the increase of NO_2-N concentration was statistically significant (One-way ANOVA, p value <0.05), whereas NH_4-N concentration decreased from surface to bottom water. The DOC concentration in the bottom layer was significantly lower than that in the surface layer (Multiple *t*-tests, q value <0.00001). The amount of POC and PON decreased vertically from surface to middle layer, but increased slightly again in the bottom water, possibly due to sediment resuspension. Moreover, the total prokaryotic abundance also decreased significantly with increasing depth (One-way ANOVA, $p <$ 0.0001).

3.2. The compositions and transcripts of microbial community

The microbial composition with phylum and family taxonomy was shown in Fig. 2. High-throughput sequencing of the 16S rRNA gene yielded 6918 OTUs that belong to 45 phyla, of which Proteobacteria (49.2%), Bacteroidetes (10.8%), Planctomycetes (5.3%), Actinobacteria (5.1%), and Verrucomicrobia (1.4%) were the predominant heterotrophic groups (Fig. 2a and Table S3). As the dominant photoautotrophic and chemolithoautotrophic groups, Cyanobacteria and Thaumarchaeota, respectively, accounted for 15.9% and 8.1% of the total microbial abundance (Fig. 2a and Table S3). While Nitrospinae and Nitrospirae, the nitrite-oxidizing bacteria, only accounted for 0.3% and 0.02%, respectively (Fig. 2a and Table S3). The above mentioned nine dominant phyla accounted for 95.9% of the total relative abundance, with the remaining 36 phyla only accounting for 4.1%. The relative proportion of Thaumarchaeota increased significantly from surface to bottom water ($p < 0.01$), while the relative proportion of Cyanobacteria decreased significantly ($p < 0.01$, Fig. 3a).

The absolute quantification of 16S rRNA genes identified 45 phyla in total. The total abundance in surface water was higher than that in the bottom, which was consistent with the trend of the total prokaryotic abundance as measured by flow cytometry (Fig. S1 and Table 1). The dominant phyla primarily included Proteobacteria (average value, 1.4×10^6 copies ml^{-1}), Cyanobacteria (3.7×10^5 copies ml^{-1}), Bacteroidetes (2.7×10^5 copies ml^{-1}), Thaumarchaeota (1.9×10^5 copies ml^{-1}), Actinobacteria (1.5×10^5 copies ml^{-1}), Planctomycetes (5.5×10^4 copies ml^{-1}), Verrucomicrobia (2.4×10^3 copies ml^{-1}), Nitrospinae (489.2 copies ml^{-1}), and Nitrospinae (12.2 copies ml^{-1}) (Fig. 2b). Among these dominant phyla, Proteobacteria, Cyanobacteria and Thaumarchaeota account for 54.7%, 14.9% and 7.6% of the total abundance, respectively (Table S3). The absolute abundance of the dominant bacteria, including Proteobacteria and Cyanobacteria, both decreased with increasing water depth, while Thaumarchaeota, Nitrospinae, and Nitrospirae showed an inverse distribution pattern (Fig. 3b). There were no significant effects of depth and DO concentration on the diversity of the dominant phyla (Fig. 3b).

At the family phylogenetic level, we obtained Family_II (9.9%, 3.3×10^5 copies ml^{-1}) in Cyanobacteria; Nitrosopumilaceae (8.1%, 1.9×10^5 copies ml^{-1}) in Thaumarchaeota; Pelagibacteraceae (9.2%, 3.8×10^5 copies ml^{-1}), Rhodobacteraceae (6.4%, 2.2×10^5 copies ml^{-1}), and Alteromonadaceae (6.3%, 1.1×10^5 copies ml^{-1}) in Proteobacteria; Flavobacteriaceae (4.4%, 1.3×10^5 copies ml^{-1}) in Bacteroidetes; Planctomycetaceae (3.3%, 3.3×10^4 copies ml^{-1}) in Planctomycetes (Fig. 2d and e). However, their relative and absolute abundance showed no significant variation with decreasing oxygen concentration (Table S4).

Using the 16S rRNA ASVs analysis, we obtained a similar microbial structure with the OTUs analysis. Furthermore, there were eight ASV species in Thaumarchaeota (Table S5), with the close similarity to cultured *Nitrosopumilus cobalaminigenes* HCA1 or *Nitrosopumilus oxyclinae* HCE1, both of which belong to the coastal ecotypes of ammonia oxidation archaea (AOA, Qin et al., 2017; Qin et al., 2020). Of these, ASV1, with the highest abundance (1.5×10^3 copies ml^{-1}) in Thaumarchaeota, was close to *Nitrosopumilus cobalaminigenes* HCA1. Additionally, some autotrophic bacteria with relatively low abundances were also observed in low oxygen samples, such as SUP05 and SAR324 (Table S5).

The metatranscriptome sequence analysis and the absolute quantification-based 16S rRNA gene amplicon sequences obtained a similar result in terms of predominant taxonomic composition at the phylum and family levels (Fig. 2 and Fig. 3). As water depth increased and DO concentration decreased, the transcriptional activity of Thaumarchaeota, especially the family Nitrosopumilaceae, significantly increased (Table S4) and that of Cyanobacteria significantly decreased ($p < 0.001$, Fig. 2c and Fig. 3c). The transcriptional activity in the bacterial community such as the families Pelagibacteraceae and Alteromonadaceae increased slightly in the bottom water (Fig. 2f and Table S4).

According to the results from 16S rRNA genes sequencing and transcriptional analysis, the taxa composition was similar between free-living and particle-associated fractions. However, the predominant phyla, including Thaumarchaeota, Proteobacteria, Actinobacteria, and Verrucomicrobia displayed significant differences ($p < 0.05$), with both higher abundance and transcriptional activity in the free-living fraction (Fig. S2).

Of the measured environmental factors, DO, pH, temperature, water depth, DIN, DIP, and DSi concentration, played a significant role in regulating the composition and transcriptional activity of the microbiomes in the low oxygen waters of the Bohai Sea (Mantel's $r > 0.5$, $p < 0.001$). The transcriptional activity of Thaumarchaeota, Nitrospinae, and Nitrospirae were significantly and negatively correlated with DO, pH, and temperature, while those of Cyanobacteria showed positive correlations to the three factors (Fig. 4). In addition, the transcriptional activity of Thaumarchaeota and Cyanobacteria showed a positive and negative correlation, respectively, to water depth (Fig. 4), indirectly implying regulations by DO and light on microbial distributions. The transcripts of Thaumarchaeota showed a negative correlation with NH_4-N concentration, and the transcripts of Nitrospinae and Nitrospirae positively correlated to NO_3-N concentration (Mantel's $r > 0.5$, $p < 0.001$, Fig. 4). These correlations directly indicated that the transcripts' functional composition was also significantly affected by the DIN concentration. Nitrosopumilaceae, the dominant family clade of Thaumarchaeota, was negatively affected by DO, pH and temperature, but positively affected by water depth, NO_3^-, DIP, and DSi concentrations (Fig. S3).

In summary, with decreasing DO, the abundance of heterotrophic bacteria (Proteobacteria and Bacteroidetes) generally decreased, but their transcriptional activity increased; both the abundance and activity of chemolithoautotrophs (Thaumarchaeota) increased, but those of photoautotrophs (Cyanobacteria) decreased. Importantly, for the family Nitrosopumilaceae (phylum Thaumarchaeota), the transcriptional activity significantly increased, implying the alteration of dominant microbial groups involved in the carbon and nitrogen cycles of low oxygen environments.

3.3. Functional diversity of microbial community

Transcriptional analysis revealed three dominant microbial lifestyles in the deoxygenated Bohai seawater: (a) photoautotrophy (Cyanobacteria: Family_II), (b) chemoautotrophy (Thaumarchaeota: Nitrosopumilaceae), and (c) heterotrophy (Rhodobacteraceae, Halieaceae, Bacteroidetes: Flavobacteriaceae, Planctomycetes: Planctomycetaceae). According to the analysis of clusters of orthologous groups (COGs), transcripts from Thaumarchaeota and Cyanobacteria showed the greatest distribution in 'energy generation and transformation' (Fig. S4). In the phylum Proteobacteria, high gene expression profile was observed in COG categories such as 'translation, ribosome structure and biogenesis' and 'post-translational modification, protein turnover, chaperone' (Fig. S4). Therefore, we primarily focused on the nitrogen metabolism and carbon fixation pathways of different microorganisms. Nitrogen metabolism in Thaumarchaeota was expressed as ammonia transportation and assimilation. Key transcripts of nitrogen metabolic pathways, such as *amoABC* (ammonia monooxygenase subunits, Gillies et al., 2015) and *nirK* (nitrite reductase, Walker et al., 2010) increased significantly as DO concentration decreased in deep water (Fig. 5a and Table S2). For carbon fixation, the transcripts of the 3-hydroxypropionic acid/4-hydroxybutyric acid cycle (the 3-HP/4-HB cycle) in Thaumarchaeota increased, but those of the Calvin-Benson-Bassham (CBB) cycle in Cyanobacteria decreased in the low oxygen waters (Fig. 5b and Fig. S5). Contrastingly, transcripts of various transporter-encoding genes, including those of ATP-binding cassette (ABC) transporters-, TonB-dependent transporters- (TBDT), and DON transporters-encoding

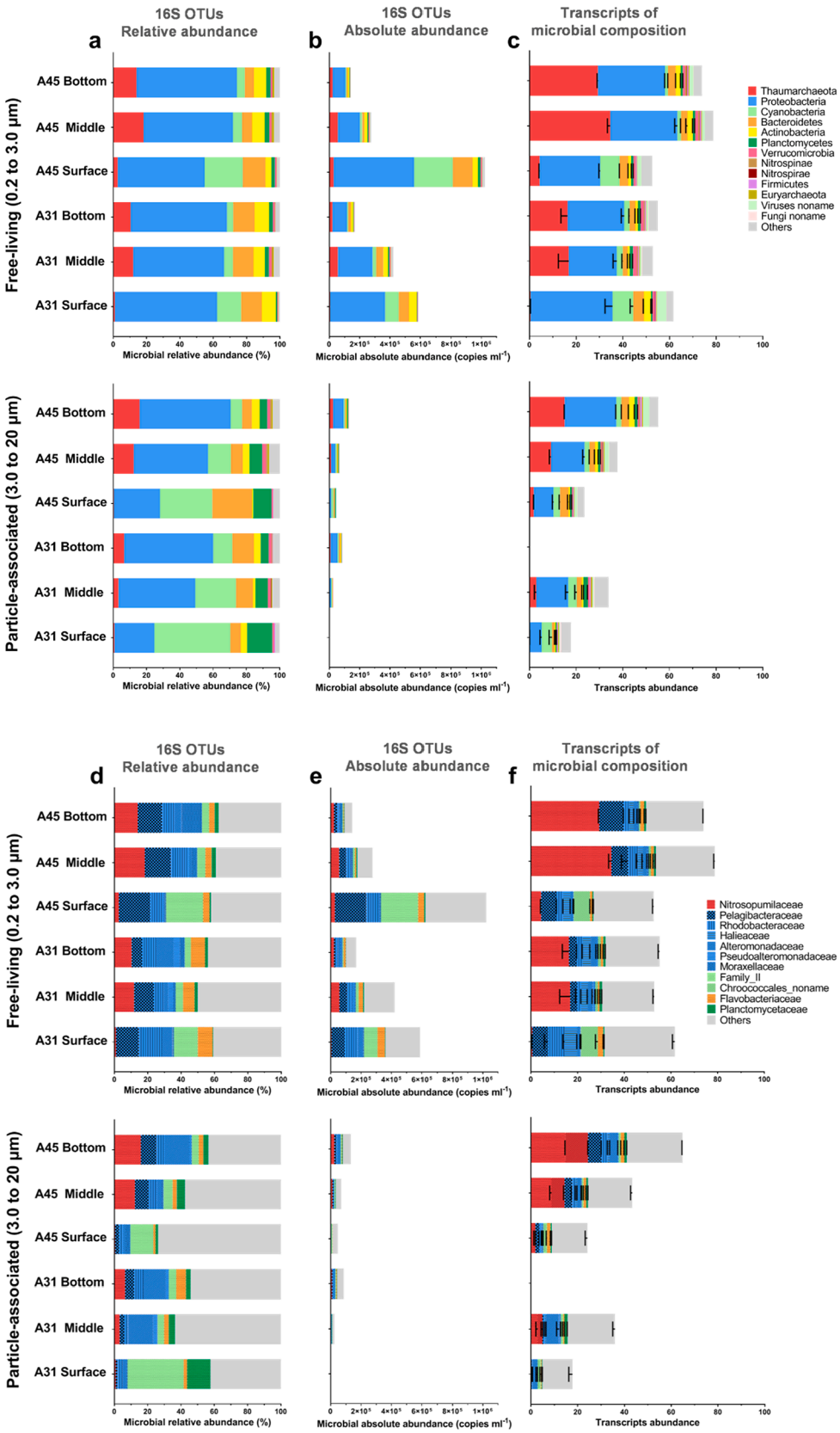

Fig. 2. Bar graph of microbial composition with phylum (a–c) and family (e–f) taxonomy for the free-living (0.2–3.0 μm) and particle-associated (3.0 to 20 μm) prokaryotic assemblages at sites A31 and A45. The relative 16S rRNA gene sequence data (a and d), the absolute quantified 16S rRNA gene sequence data (b and e), and the taxonomy of transcripts (c and f) reflect the dynamics of microbial composition in surface, middle, and bottom layers. Less abundant groups were summed and assigned as 'Others'. The error bars represent the standard deviation of triplicates.

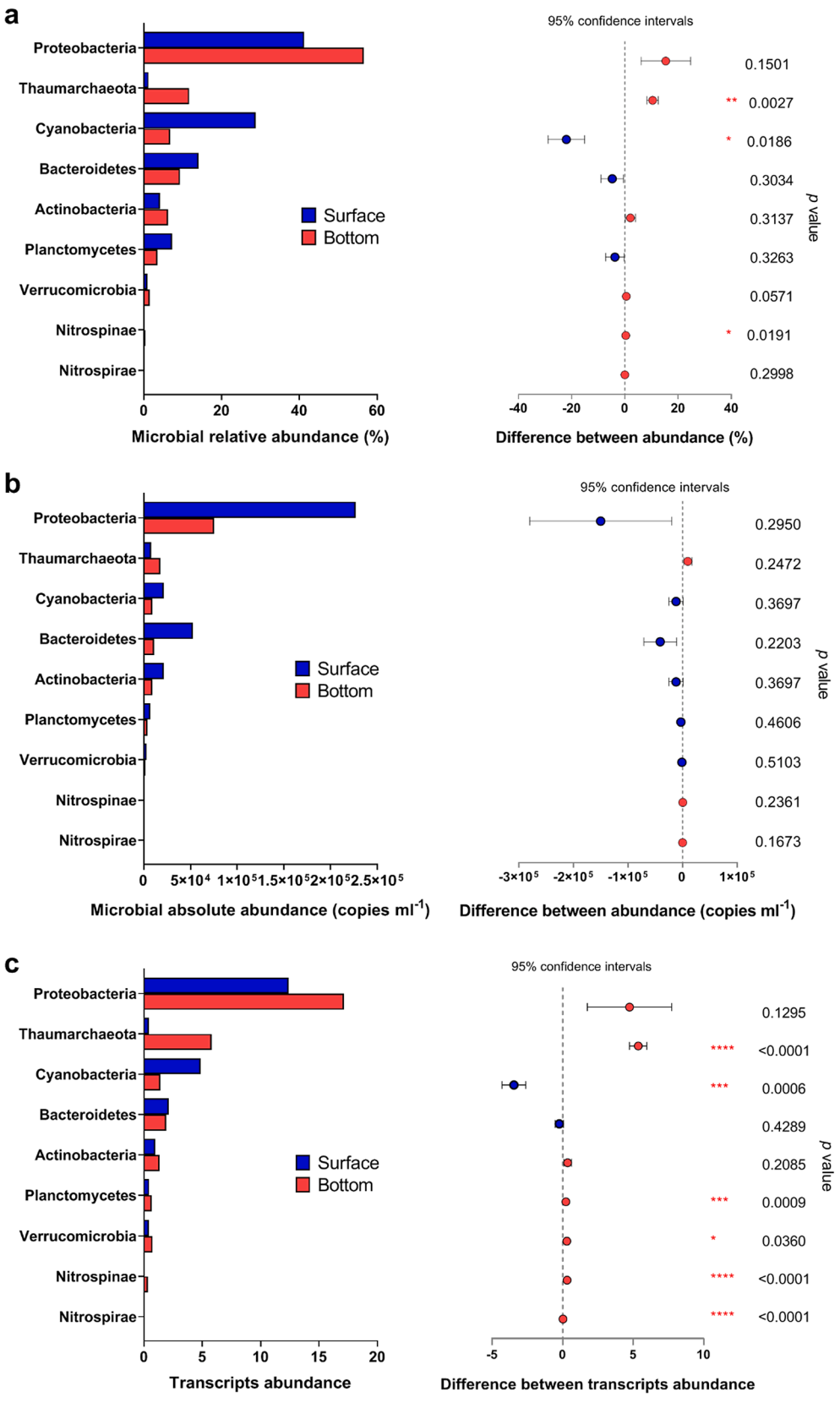

Fig. 3. The variation of dominant microbial groups in the surface and bottom seawater in low oxygen areas. The abundance and difference for the relative 16S rRNA gene sequence data (a), the absolute quantified 16S rRNA gene sequence data (b), and the taxonomy of transcripts (c) were shown. The differences were analyzed using Student's *t*-test at 95% confidence interval and the *p* values were also listed. *, **, *** and **** denote *p* value less than 0.05, 0.01, 0.001, and 0.0001, respectively.

genes (especially those involved in the transport of amino acids, peptides, nucleosides, and vitamins), showed high abundance among heterotrophic bacteria in low DO water (Fig. 6 and Fig. S6). 3199 genes encoding for substrate-binding protein of ABC transporter were expressed and predicted to transport amino acids, peptides, nucleosides, polyamines, carbohydrates and glycine betaine (Table S6). Similarly, 3842 genes encoding for TonB-dependent transporter were expressed and predicted to transport siderophores and/or vitamin B12 (Table S6).

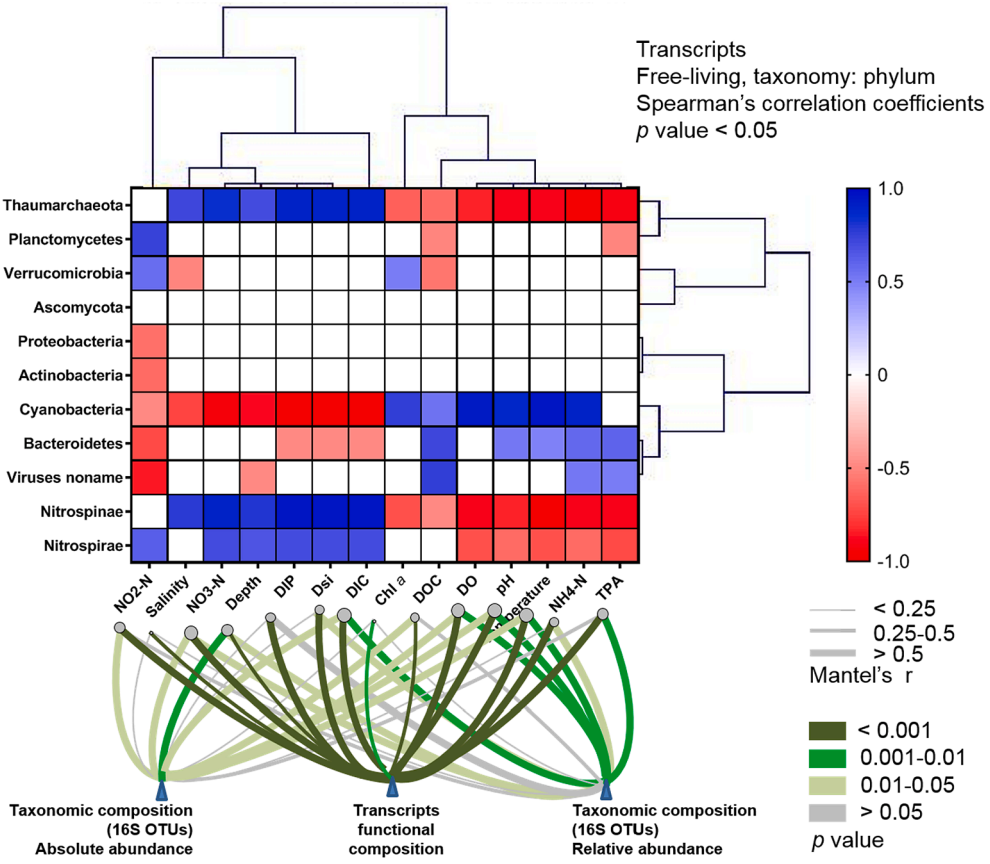

Fig. 4. Environmental drivers of microbial community composition in deoxygenated ocean. Heatmap shows the comparisons between environmental factors and the dominant microbial groups (taxonomy in family), with a color gradient denoting Spearman's correlation coefficient. Taxonomic (absolute and relative abundance) and transcript functional community compositions were related to each environmental factor by Mantel partial tests. Edge width corresponds to the Mantel's r statistic for the corresponding distance correlations, and edge color denotes the statistical significance based on 9,999 permutations.

Relative to the particle-associated assemblage, free-living microbes expressed higher transporter-related transcripts. The total expression of transcripts in the free-living community was highest in the surface water, while those in particle-associated community showed an inverse trend with high transcript in the bottom water (Fig. 6). Higher levels of transcripts related to the antioxidant abilities of Thaumarchaeota, such as the superoxide dismutase and an inefficient hydrogen peroxide scavenging coding gene (peroxiredoxin), were observed in the bottom layer with its associated low DO concentration regardless of free-living or particulate-associated lifestyle (Fig. 7).

4. Discussion

4.1. Autotrophic carbon fixation and ammonia oxidation in deoxygenated waters

We observed high abundance and transcriptional activity of Thaumarchaeota in the low oxygen coastal zone (Fig. 2). Similar results were also found in hypoxic zones (Gillies et al., 2015; Plominsky et al., 2018), suggesting that Thaumarchaeota may play a more important ecological function in deoxygenation zones. The transcripts of *amoABC*-encoding genes for Thaumarchaeota, the core coding genes of the ammonia oxidation pathway regarding energy metabolism (NH_4-N oxidation and NO_2-N production) (Kerou et al., 2016), were significantly increased by 5–21 folds in low DO waters ($p < 0.001$, Fig. 5a and Table S2). The combination of declining NH_4-N concentration and rising NO_2-N concentration with water depth in the surrounding water environment (Table 1), strongly indicated that the active Thaumarchaeota have an important role in regulating the distribution pattern of different inorganic nitrogen species. Another significantly increased transcript, the NO-forming nitrite reductase-encoding gene (*nirK*) (10-folds, $p < 0.0001$, Fig. 5a and Table S2), was previously suggested to assist in the ammonia oxidation process (Kozlowski et al., 2016; Schleper and Nicol, 2010; Walker et al., 2010), as NO, the product of the *nirK* reaction, is vital to ammonia oxidation (Kerou et al., 2016; Kozlowski et al., 2016; Sauder et al., 2016; Shen et al., 2013). The high transcription activity of Thaumarchaeota in low oxygen waters may suggest an increased demand for NH_4-N (Han et al., 2021; Hong et al., 2015). We found a significant increase (8–22 folds, $p < 0.001$, Fig. 5a and Table S2) in the transcripts of ammonia transporter-encoding genes (*amt*, Amt family transporters), which are dedicated to increase ammonia transport when passive diffusion is limited by low ammonia availability, low extracellular pH, or low permeability of the cytomembrane (Offre et al., 2014; Winkler, 2006). Moreover, we observed a significant increase in transcription of glutamine synthetase-, glutamate dehydrogenase-, and aspartate ammonia-lyase-encoding genes (Fig. 5a and Table S2), implying that Thaumarchaeota could obtain ammonia via organic matter decomposition (Kerou et al., 2016). In addition, the PII superfamily (encoded by *glnB*) is a key player in regulating nitrogen transfer in microbes (Huergo et al., 2013; Kerou et al., 2016), the increase transcripts of this coding gene in Thaumarchaeota suggest active nitrogen transformation processes in the hypoxic zones. However, the presence and function of urea transporters- and urease-coding genes were not detected in this Thaumarchaeotal group, even though urea has been reported to be a substrate for nitrification (Kitzinger et al., 2019). The 3-HP/4-HB cycle is far more energy efficient than aerobic autotrophic pathways (such as the CBB cycle, Könneke et al., 2014). The transcripts in relation to this chemoautotrophic carbon fixation pathway in Thaumarchaeota increased by 6–33 folds in low oxygen waters (Fig. 5b and Table S2). The acetyl-CoA/propionyl-CoA carboxylase (Berg et al., 2010; Hügler et al., 2003), 3-hydroxypropionyl-coenzyme A dehydratase, and 4-hydroxybutyryl-CoA dehydratase (Berg et al., 2007; Hügler and Sievert, 2011; Könneke et al., 2014) are the main coding genes regulating the 3-HP/4-HB cycle, and the transcripts of these

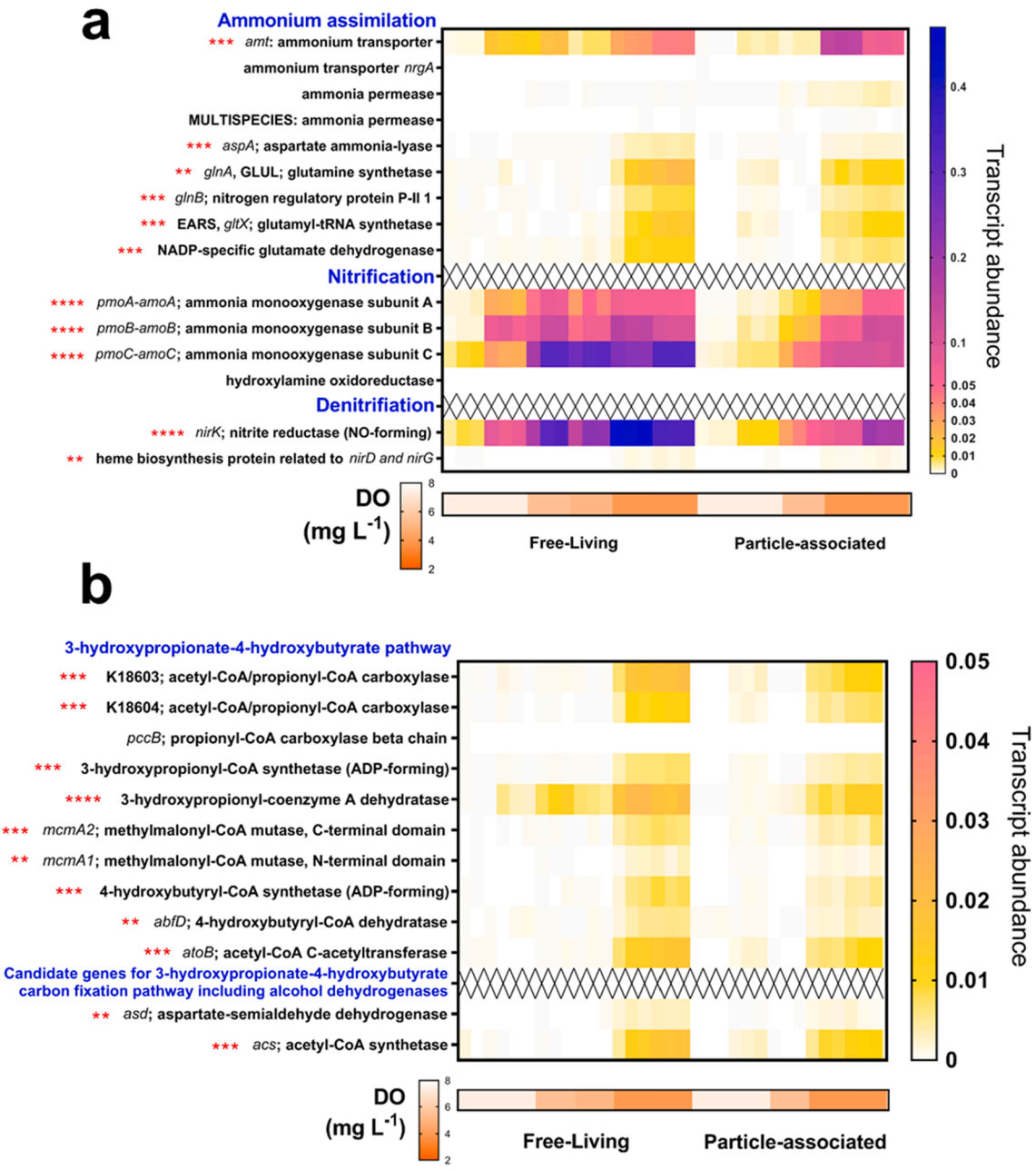

Fig. 5. Transcript abundance of selected core coding genes in free-living (0.2–3.0 μm) and particle-associated (3.0–20 μm) assemblages of Thaumarchaeota that involved in (a) nitrogen and (b) carbon metabolism in the deoxygenated costal ocean. The predicted transcripts are grouped into ammonium assimilation, nitrification, denitrification, and 3-hydroxypropionic acid/4-hydroxybutyric acid cycle. The confidence for significant differences between the surface and bottom seawaters are denoted by *, **, *** and ****, for *p* value less than 0.05, 0.01, 0.001, and 0.0001, respectively.

coding genes all significantly increased in bottom low oxygen waters ($p < 0.01$, Fig. 5b). In particular, Thaumarchaeotal 4-hydroxybutyryl-CoA dehydratase has a low sensitivity to oxygen and can maintain higher enzyme activity under low oxygen conditions (Demirci et al., 2020). These high transcript levels of chemoautotrophic carbon fixation may provide a plausible biochemical explanation for the thriving Thaumarchaeota population within deoxygenated environments. A significant decrease in Cyanobacterial abundance and transcription of genes related to photosynthesis, including photosystem I P700 chlorophyll an apoprotein- (*psa* family genes) and photosystem II P680 reaction center protein-encoding genes (*psb* family genes, López-Gomollón et al., 2007), was observed with increasing water depth, decreasing light levels and oxygen concentration (Table S2). For example, the characteristic coding gene of ribulose 1,5-bisphosphate carboxylase/oxygenase (RuBisCO), a core coding gene involved in the CBB cycle, a major carbon fixation pathway for Cyanobacteria (Hügler and Sievert, 2011), also significantly decreased by 9-folds in deep waters ($p < 0.05$, Fig. S5 and Table S2). The RuBisCO-coding gene in Cyanobacteria, particularly in *Synechococcus*, were abundantly expressed in the oxygen rich surface waters which are exposed to high light levels (Table S2). While in the deep water, the transcripts of RuBisCO were abundant in chemoautotrophs, especially Nitrosomonas and Nitrosospira of Proteobacteria, and Acidithiomicrobium of Actinobacteria (Table S2). This indicated that the pattern of carbon fixation shifted from photoautotrophy to chemoautotrophy in the deoxygenated zone.

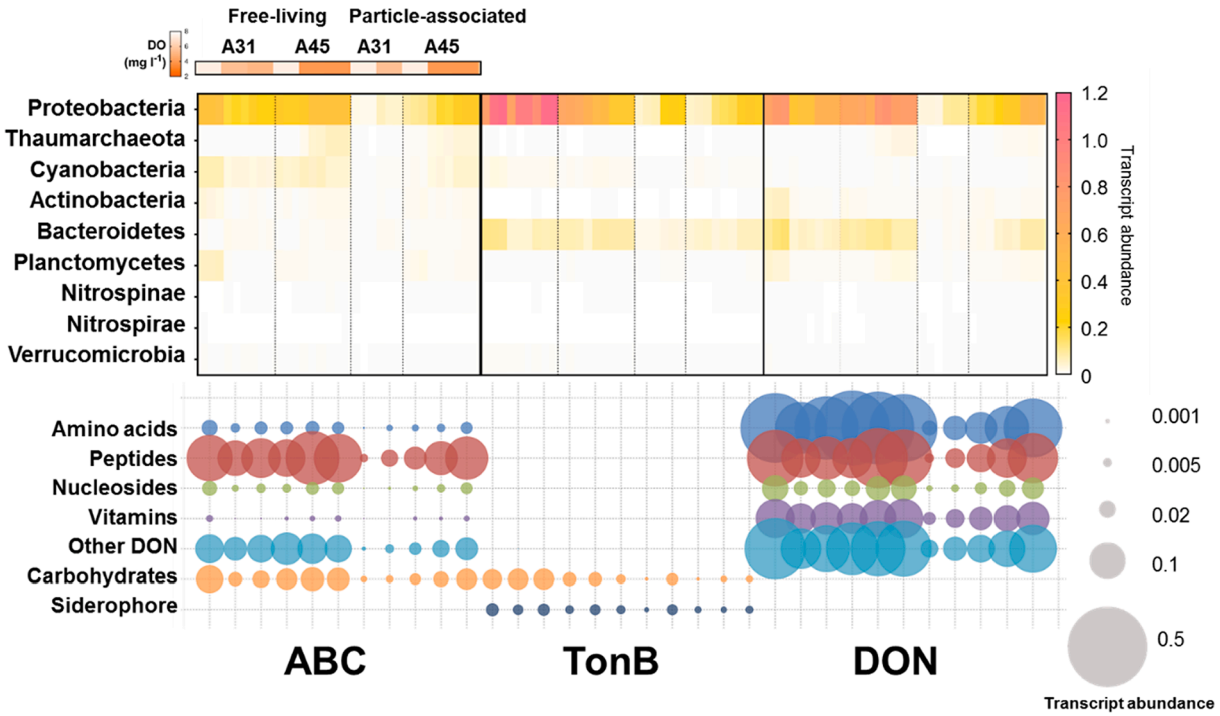

Fig. 6. Transcript abundance of selected transporters of dominant microbial groups in the deoxygenated costal ocean. The coding genes of transporters are grouped into the ATP-binding cassette transporters (ABC), TonB-dependent transporters (TonB), and the predicted dissolved organic nitrogen transporters (DON). The heatmap shows the variation in expression of transporter-encoding genes among different dominant groups. The size of solid circle denotes the abundance of transcripts for transporter-coding genes. The samples are divided into free-living (0.2–3.0 μm) and particle-associated (3.0–20 μm) assemblages.

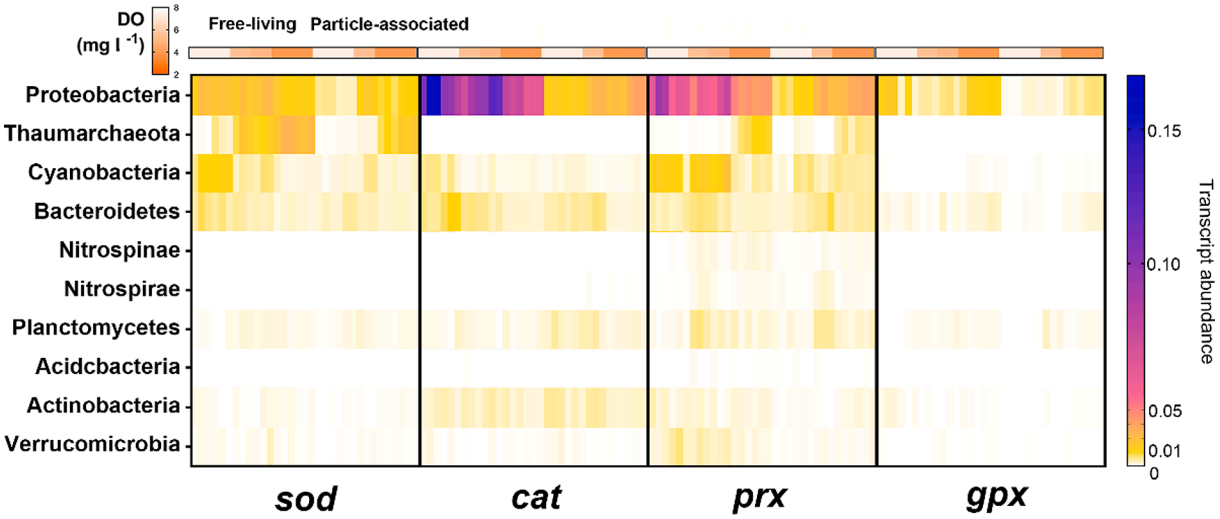

Fig. 7. Transcript abundance of antioxidant coding genes in the dominant groups in the deoxygenated costal ocean. The predicted transcripts are grouped into superoxide dismutase (*sod*), catalase (*cat*), peroxiredoxin (*prx*), glutathione peroxidase (*gpx*). The samples are divided into free-living (0.2–3.0 μm) and particle-associated (3.0–20 μm) assemblages.

4.2. Uptake of organic nitrogen by microbes

Heterotrophic bacteria transcribed abundant transporter-encoding genes, including ABC transporters, and TBDTs and DON related transporters in the deoxygenated coastal seawater (Fig. 6). Among the various transporter-encoding genes, the families Pelagibacteraceae and Rhodobacteraceae in Proteobacteria expressed abundant transcripts of ABC transporter-encoding genes for the transport of nitrogen-containing organics, including amino acids, peptides, polyamines, nucleosides, glycine betaine (Fig. 6 and Table S6). While the families Halieaceae and Alteromonadaceae in Proteobacteria and the family Flavobacteriaceae in Bacteroidetes expressed high transcription of TBDT- and DON transporter-encoding genes (Fig. 6). In particular, the normalized transcript of DON transporter-encoding genes increased with decreasing DO concentration (Fig. S6). The transcripts of TBDT transporter-encoding genes generally functioned in the transport of siderophore and vitamin B12. The transcripts of DON transporter-encoding genes are responsible for the transportation of amino acids, peptides, nucleosides, and vitamins. *susC* and *susD* are key genes for recognition and binding of high molecular weight compounds such as polysaccharides and oligosaccharides (Tang et al., 2017). The transcripts of these two key genes were almost unobserved in this study (Table S6), implying that microbes in

low oxygen environments may prefer to metabolize low-molecular-weight compounds. Heterotrophic bacteria can take up low-molecular-weight DON and release ammonia to the environment (Han et al., 2021). Extracellular NH_4-N supplementation plays an important role in supporting Thaumarchaeotal oxidation of ammonia (Hong et al., 2015). Moreover, both the transcription of ABC transporter- and DON transporter-encoding genes increased significantly in the bottom deoxygenated seawater, indicating a mixotrophic lifestyle for Thaumarchaeota in the low oxygen seawater (Qin et al., 2014). In terms of the normalized transcript, the transcripts of all related transporter-encoding genes increased in the free-living community, but decreased in the particle-associated community with depth (Fig. S6), indicating a free-living-preferred lifestyle for dominant microbes such as Proteobacteria and Thaumarchaeota in low oxygen waters.

4.3. Dynamics of antioxidant coding genes across an oxygen gradient

We also focused on the transcriptional activity of antioxidant coding genes from major microbial groups in the deoxygenated regions. Reactive oxygen molecules (ROS), including superoxide and hydrogen peroxide (H_2O_2), can be intracellularly produced during photosynthesis and microbial respiration (Zinser, 2018a), or extracellularly generated during photodegradation (Heller et al., 2016; Song and Jiang, 2020) and extracellular superoxide production (Diaz et al., 2013; Sutherland et al., 2019; Sutherland et al., 2020), resulting in oxidative damage to proteins, DNA, and lipids in microbes when a critical ROS concentration is reached (Zinser, 2018b). Microorganisms deal with ROS mainly through superoxide dismutase (*sod*), two types of catalase (*cat*), peroxiredoxin (*prx*), and glutathione peroxidase (*gpx*) (Heller and Croot, 2010; Mishra and Imlay, 2012; Petasne and Zika, 1987). Nanomolar levels of H_2O_2 might inhibit the growth of Thaumarchaeota (Tolar et al., 2016), due to the lack or partial loss of *cat* to scavenge it (Bayer et al., 2019; Ma et al., 2017; Zinser, 2018b). We found that with decreasing concentration of DO, the abundance of antioxidant transcripts (including *sod* and *cat*) in heterotrophic bacteria and Cyanobacteria in the bottom water was lower than that at the surface (Fig. 7). However, the transcripts of *sod* and the low-efficiency peroxide scavenging coding gene *prx* in Thaumarchaeota increased by ~13-fold in low oxygen waters regardless of lifestyles, but no transcripts of *cat* were detected (Fig. 7 and Table S2), even though the scavenging of H_2O_2 with *cat* is 100–1000 times more efficient than that with *prx* (Parsonage et al., 2008). However, the normalized transcripts of antioxidant coding genes in dominant microbes gradually increased along with the declining oxygen concentration (Fig. S7a), corresponding to the increased transcripts of electron transfer chain coding genes (Complex I, II, III, and IV, Fig. S7b). A decrease in DO concentration resulted in the increased chemoautotrophic and heterotrophic production of a marine environment (Suter et al., 2020). The enhanced metabolic activities in low oxygen environments may lead to a high level of intracellular ROS production (Hansel et al., 2019). In this study, the elevated normalized transcripts of antioxidant coding genes in Thaumarchaeota in low oxygen water are a response to the intracellularly produced ROS stress as a result of the active ammonia oxidation process (see high normalized transcripts of *amoABC* coding gene in Fig. S7c). In addition, both decreased light and decreased total abundance of photoautotrophs and microorganisms in bottom water, results in a decline of associated extracellular ROS production (Song and Jiang, 2020; Sutherland et al., 2020), and subsequently mitigating the pressure on survival of Thaumarchaeota in low oxygen conditions (Tolar et al., 2016). Moreover, the 16S rRNA ASVs analysis indicated that the costal ecotypes of Thaumarchaeota are more resilient to ROS stress than the open-ocean ecotypes (Qin et al., 2020; Tolar et al., 2016). Collectively, these findings may partially explain why the Thaumarchaeota population is sustained in deoxygenated regions.

5. Conclusions

We observed high transcriptional activity of Thaumarchaeota in the deoxygenated waters, with significant increase in the expression of core genes representing ammonia oxidation, ammonia transport, and carbon fixation pathways. Meanwhile, the transcripts of Cyanobacteria (particularly for photosynthesis and carbon fixation) significantly decreased. The transcripts of RuBisCO shifted from photoautotrophy to chemoautotrophy in bottom water with low DO concentration. Moreover, the transcription profile of heterotrophic bacteria indicated that heterotrophs play a major role in transforming low-molecular-weight DON. The elevated normalized transcripts of antioxidant coding genes correspond to an enhanced aerobic metabolism of Thaumarchaeota in the low oxygen seawater. Generally, our findings indicate that Thaumarchaeota, especially the coastal ecotypes capable of ammonia-oxidization, have a great resilience to low oxygen aquatic environments, and their chemolithoautotrophic carbon fixation contributes greatly to the carbon flow under such environmental conditions.

CRediT authorship contribution statement

Yu Han: Investigation, Methodology, Formal analysis, Writing – original draft, Writing – review & editing. **Mu Zhang:** Project administration, Formal analysis, Writing – review & editing, Supervision. **Xiaofeng Chen:** Writing – review & editing. **Weidong Zhai:** Methodology, Writing – review & editing. **Ehui Tan:** Writing – review & editing. **Kai Tang:**.

Declaration of Competing Interest

The authors declare that they have no known competing financial interests or personal relationships that could have appeared to influence the work reported in this paper.

Acknowledgements

We thank Liwen Zheng, Siqing Yu and Yubin Hu in Shandong University (Qingdao) for the data of DO, pH and nutrients, and we thank Jiang Tao and Guowang Yan in the Yellow Sea Fisheries Research Institute for the data of Chl *a*.

Funding

This work was supported by the National Key Research and Development Program of China (2020YFA0608300), the National Natural Science Foundation of China project (41776167, 42076160, 91751207, 41861144018), and International Science Partnership Program of the Chinese Academy of Sciences (121311KYSB20190029).

Ethical approval

This article does not contain any studies with human participants or animals performed by any of the authors.

Appendix A. Supplementary material

Supplementary data to this article can be found online at https://doi.org/10.1016/j.envint.2021.106889.

References

Bayer, B., Pelikan, C., Bittner, M.J., Reinthaler, T., Könneke, M., Herndl, G.J., Offre, P., 2019. Proteomic response of three marine ammonia-oxidizing archaea to hydrogen peroxide and their metabolic interactions with a heterotrophic alphaproteobacterium. mSystems 4 e00181–e00119.

Benson, B.B., Krause, D., 1984. The concentration and isotopic fractionation of oxygen dissolved in freshwater and seawater in equilibrium with the atmosphere. Limnol. Oceanogr. 29 (3), 620–632.
Berg, I.A., Kockelkorn, D., Buckel, W., Fuchs, G., 2007. A 3-Hydroxypropionate/4-hydroxybutyrate autotrophic carbon dioxide assimilation pathway in archaea. Science 318 (5857), 1782–1786.
Berg, I.A., Kockelkorn, D., Ramos-Vera, W.H., Say, R.F., Zarzycki, J., Hügler, M., Alber, B.E., Fuchs, G., 2010. Autotrophic carbon fixation in archaea. Nat. Rev. Microbiol. 8 (6), 447–460.
Bokulich, N.A., Kaehler, B.D., Ram, R.J., Matthew, D., Evan, B., Rob, K., Huttley, G.A., Gregory, C.J., 2018. Optimizing taxonomic classification of marker-gene amplicon sequences with QIIME 2's q2-feature-classifier plugin. Microbiome 6, 90.
Bolyen, E., Rideout, J.R., Dillon, M.R., Bokulich, N.A., Abnet, C.C., Al-Ghalith, G.A., Alexander, H., Alm, E.J., Arumugam, M., Asnicar, F., Bai, Y., Bisanz, J.E., Bittinger, K., Brejnrod, A., Brislawn, C.J., Brown, C.T., Callahan, B.J., Caraballo-Rodríguez, A.M., Chase, J., Cope, E.K., Da Silva, R., Diener, C., Dorrestein, P.C., Douglas, G.M., Durall, D.M., Duvallet, C., Edwardson, C.F., Ernst, M., Estaki, M., Fouquier, J., Gauglitz, J.M., Gibbons, S.M., Gibson, D.L., Gonzalez, A., Gorlick, K., Guo, J., Hillmann, B., Holmes, S., Holste, H., Huttenhower, C., Huttley, G.A., Janssen, S., Jarmusch, A.K., Jiang, L., Kaehler, B.D., Kang, K.B., Keefe, C.R., Keim, P., Kelley, S.T., Knights, D., Koester, I., Kosciolek, T., Kreps, J., Langille, M.G.I., Lee, J., Ley, R., Liu, Y.-X., Loftfield, E., Lozupone, C., Maher, M., Marotz, C., Martin, B.D., McDonald, D., McIver, L.J., Melnik, A.V., Metcalf, J.L., Morgan, S.C., Morton, J.T., Naimey, A.T., Navas-Molina, J.A., Nothias, L.F., Orchanian, S.B., Pearson, T., Peoples, S.L., Petras, D., Preuss, M.L., Pruesse, E., Rasmussen, L.B., Rivers, A., Robeson, M.S., Rosenthal, P., Segata, N., Shaffer, M., Shiffer, A., Sinha, R., Song, S.J., Spear, J.R., Swafford, A.D., Thompson, L.R., Torres, P.J., Trinh, P., Tripathi, A., Turnbaugh, P.J., Ul-Hasan, S., van der Hooft, J.J.J., Vargas, F., Vázquez-Baeza, Y., Vogtmann, E., von Hippel, M., Walters, W., Wan, Y., Wang, M., Warren, J., Weber, K. C., Williamson, C.H.D., Willis, A.D., Xu, Z.Z., Zaneveld, J.R., Zhang, Y., Zhu, Q., Knight, R., Caporaso, J.G., 2019. Reproducible, interactive, scalable and extensible microbiome data science using QIIME 2. Nat. Biotechnol. 37 (8), 852–857.
Breitburg, D., Levin, L.A., Oschlies, A., Grégoire, M., Chavez, F.P., Conley, D.J., Garçon, V., Gilbert, D., Gutiérrez, D., Isensee, K., Jacinto, G.S., Limburg, K.E., Montes, I., Naqvi, S.W.A., Pitcher, G.C., Rabalais, N.N., Roman, M.R., Rose, K.A., Seibel, B.A., Telszewski, M., Yasuhara, M., Zhang, J., 2018. Declining oxygen in the global ocean and coastal waters. Science 359 (6371), eaam7240. https://doi.org/10.1126/science:aam7240.
Cai, W.J., Dai, M., Wang, Y., Zhai, W., Huang, T., Chen, S., Zhang, F., Chen, Z., Wang, Z., 2004. The biogeochemistry of inorganic carbon and nutrients in the Pearl River estuary and the adjacent Northern South China Sea. Continental Shelf Research 24, 1301–1319.
Cai, R., Zhou, W., He, C., Tang, K., Guo, W., Gonsior, M., Jiao, N., 2019. Microbial processing of sediment-derived dissolved organic matter: Implications for its subsequent biogeochemical cycling in overlying seawater. J. Geophys. Res.: Biogeoences 124 (11), 3479–3490.
Callahan, B.J., McMurdie, P.J., Holmes, S.P., 2017. Exact sequence variants should replace operational taxonomic units in marker-gene data analysis. ISME J. 11 (12), 2639–2643.
Chen, C.-C., Gong, G.-C., Shiah, F.-K., 2007. Hypoxia in the East China Sea: One of the largest coastal low-oxygen areas in the world. Mar. Environ. Res. 64 (4), 399–408.
Dai, M., Wang, L., Guo, X., Zhai, W., Li, Q., He, B., Kao, S.-J., 2008. Nitrification and inorganic nitrogen distribution in a large perturbed river/estuarine system: the Pearl River Estuary, China. Biogeosciences 5 (5), 1227–1244.
Demirci, H., Tolar, B.B., Doukov, T., Petriceks, A., Wakatsuki, S. (2020) Structural adaptation of oxygen tolerance in 4-hydroxybutyrl-CoA dehydratase, a key enzyme of archaeal carbon fixation.
Diaz, J.M., Hansel, C.M., Voelker, B.M., Mendes, C.M., Andeer, P.F., Zhang, T., 2013. Widespread production of extracellular superoxide by heterotrophic bacteria. Science 340 (6137), 1223–1226.
Dominique, M., Frederic, P., Stephan, J., Daniel, V., 1997. Enumeration and cell cycle analysis of natural populations of marine picoplankton by flow cytometry using the nucleic acid stain SYBR Green I. Appl. Environ. Microbiol. 63, 186–193.
Fennel, K., Testa, J.M., 2019. Biogeochemical Controls on Coastal Hypoxia. Annu. Rev. Mar. Sci. 11 (1), 105–130.
Gillies, L.E., Thrash, J.C., deRada, S., Rabalais, N.N., Mason, O.U., 2015. Archaeal enrichment in the hypoxic zone in the northern Gulf of Mexico. Environ. Microbiol. 17 (10), 3847–3856.
Han, Y., Jiao, N.Z., Zhang, Y., Zhang, F., He, C., Liang, X.J., Cai, R.H., Shi, Q., Tang, K., 2021. Opportunistic bacteria with reduced genomes are effective competitors for organic nitrogen compounds in coastal dinoflagellate blooms. Microbiome 9, 71.
Hansel, C.M., Diaz, J.M., Plummer, S., 2019. Tight regulation of extracellular superoxide points to its vital role in the physiology of the globally relevant roseobacter clade. mBio 10 (2), e02668–e2718.
Heller, M.I., Croot, P.L., 2010. Superoxide decay kinetics in the Southern Ocean. Environ. Sci. Technol. 44 (1), 191–196.
Heller, M.I., Wuttig, K., Croot, P.L., 2016. Identifying the sources and sinks of CDOM/FDOM across the Mauritanian Shelf and their potential role in the decomposition of superoxide (O_2^-). Front. Mar. Sci. 3, 132.
Hewson, I., Eggleston, E.M., Doherty, M., Lee, D.Y., Owens, M., Shapleigh, J.P., Cornwell, J.C., Crump, B.C., 2013. Metatranscriptomic analyses of plankton communities inhabiting surface and subpycnocline waters of the Chesapeake Bay during oxic-anoxic-oxic transitions. Appl. Environ. Microbiol. 80 (1), 328–338.
Hong, Y., Hong, J.K., Cho, J.C., 2015. Environmental variables shaping the ecological niche of *Thaumarchaeota* in soil: Direct and indirect causal effects. PLoS One 10, e0133763.
Huang, X., Liu, L., Wen, T., Zhu, R., Zhang, J., Cai, Z., 2015. Illumina MiSeq investigations on the changes of microbial community in the *Fusarium oxysporum* f. sp. *cubense* infected soil during and after reductive soil disinfestation. Microbiol. Res. 181, 33–42.
Huergo, L.F., Chandra, G., Merrick, M., 2013. PII signal transduction proteins: Nitrogen regulation and beyond. FEMS Microbiol. Rev. 37 (2), 251–283.
Huerta-Cepas, J., Szklarczyk, D., Forslund, K., Cook, H., Heller, D., Walter, M.C., Rattei, T., Mende, D.R., Sunagawa, S., Kuhn, M., Jensen, L.J., von Mering, C., Bork, P., 2016. eggNOG 4.5: a hierarchical orthology framework with improved functional annotations for eukaryotic, prokaryotic and viral sequences. Nucleic Acids Res. 44, D286–D293.
Hügler, M., Krieger, R.S., Jahn, M., Fuchs, G., 2003. Characterization of acetyl-CoA/propionyl-CoA carboxylase in *Metallosphaera sedula*. Carboxylating enzyme in the 3-hydroxypropionate cycle for autotrophic carbon fixation. Eur. J. Biochem. 270 (4), 736–744.
Hügler, M., Sievert, S.M., 2011. Beyond the Calvin cycle: autotrophic carbon fixation in the ocean. Annu. Rev. Mar. Sci. 3 (1), 261–289.
Huson, D.H., Buchfink, B., 2015. Fast and sensitive protein alignment using DIAMOND. Nature Methods 12, 59–60.
Jessen, G.L., Lichtschlag, A., Ramette, A., Pantoja, S., Rossel, P.E., Schubert, C.J., Struck, U., Boetius, A., 2017. Hypoxia causes preservation of labile organic matter and changes seafloor microbial community composition (Black Sea). Sci. Adv. 3 (2), e1601897. https://doi.org/10.1126/sciadv.1601897.
Jiang, S.-Q., Yu, Y.-N., Gao, R.-W., Wang, H., Zhang, J., Li, R., Long, X.-H., Shen, Q.-R., Chen, W., Cai, F., 2019. High-throughput absolute quantification sequencing reveals the effect of different fertilizer applications on bacterial community in a tomato cultivated coastal saline soil. Sci. Total Environ. 687, 601–609.
Kalvelage, T., Lavik, G., Jensen, M.M., Revsbech, N.P., Loscher, C., Schunck, H., Desai, D. K., Hauss, H., Kiko, R., Holtappels, M., LaRoche, J., Schmitz, R.A., Graco, M.I., Kuypers, M.M., 2015. Aerobic microbial respiration in oceanic oxygen minimum zones. PLoS One 10, e0133526.
Kanehisa, M., Goto, S., 2000. KEGG: kyoto encyclopedia of genes and genomes. Nucleic Acids Res. 28, 27–30.
Kao, S.-J., Terence Yang, J.-Y., Liu, K.-K., Dai, M., Chou, W.-C., Lin, H.-L., Ren, H., 2012. Isotope constraints on particulate nitrogen source and dynamics in the upper water column of the oligotrophic South China Sea. Global Biogeochem. Cycles 26 (2) n/a–n/a.
Karl, D.M., 2002. Hidden in a sea of microbes. Nature 415 (6872), 590–591.
Keeling, R.F., Körtzinger, A., Gruber, N., 2010. Ocean deoxygenation in a warming world. Annu. Rev. Mar. Sci. 2 (1), 199–229.
Kerou, M., Offre, P., Valledor, L., Abby, S.S., Melcher, M., Nagler, M., Weckwerth, W., Schleper, C., 2016. Proteomics and comparative genomics of *Nitrososphaera viennensis* reveal the core genome and adaptations of archaeal ammonia oxidizers. PNAS 113 (49), E7937–E7946.
Kitzinger, K., Padilla, C.C., Marchant, H.K., Hach, P.F., Herbold, C.W., Kidane, A.T., Könneke, M., Littmann, S., Mooshammer, M., Niggemann, J., Petrov, S., Richter, A., Stewart, F.J., Wagner, M., Kuypers, M.M.M., Bristow, L.A., 2019. Cyanate and urea are substrates for nitrification by Thaumarchaeota in the marine environment. Nat. Microbiol. 4 (2), 234–243.
Konneke, M., Schubert, D.M., Brown, P.C., Hugler, M., Standfest, S., Schwander, T., Schada von Borzyskowski, L., Erb, T.J., Stahl, D.A., Berg, I.A., 2014. Ammonia-oxidizing archaea use the most energy-efficient aerobic pathway for CO_2 fixation. PNAS 111 (22), 8239–8244.
Kozlowski, J.A., Stieglmeier, M., Schleper, C., Klotz, M.G., Stein, L.Y., 2016. Pathways and key intermediates required for obligate aerobic ammonia-dependent chemolithotrophy in bacteria and Thaumarchaeota. ISME J. 10 (8), 1836–1845.
López-Gomollón, S., Hernández, J.A., Pellicer, S., Angarica, V.E., Peleato, M.L., Fillat, M. F., 2007. Cross-talk between iron and nitrogen regulatory networks in *Anabaena (Nostoc)* sp. PCC 7120: Identification of overlapping genes in FurA and NtcA regulons. J. Mol. Biol. 374 (1), 267–281.
Laffoley, D., Baxter, J.M. (Eds.), 2019. In Ocean Deoxygenation: Everyone's Problem. Causes, Impacts, Consequences and Solutions (IUCN).
Lekunberri, I., Sintes, E., de Corte, D., Yokokawa, T., Herndl, G.J., 2013. Spatial patterns of bacterial and archaeal communities along the Romanche Fracture Zone (tropical Atlantic). FEMS Microbiol. Ecol. 85 (3), 537–552.
Li, H., Handsaker, B., Wysoker, A., Fennell, T., Ruan, J., Homer, N., Marth, G., Abecasis, G., Durbin, R., 2009. The sequence alignment/map format and SAMtools. Bioinformatics 25 (16), 2078–2079.
Lombard, V., Golaconda Ramulu, H., Drula, E., Coutinho, P.M., Henrissat, B., 2013. The carbohydrate-active enzymes database (CAZy) in 2013. Nucleic Acids Res. 42, D490–D495.
Ma, L., Calfee, B.C., Morris, J.J., Johnson, Z.I., Zinser, E.R., 2017. Degradation of hydrogen peroxide at the ocean's surface: the influence of the microbial community on the realized thermal niche of *Prochlorococcus*. ISME J. 12 (2), 473–484.
Mishra, S., Imlay, J., 2012. Why do bacteria use so many enzymes to scavenge hydrogen peroxide? Arch. Biochem. Biophys. 525 (2), 145–160.
Molina, V., Belmar, L., Ulloa, O., 2010. High diversity of ammonia-oxidizing archaea in permanent and seasonal oxygen-deficient waters of the eastern South Pacific. Environ. Microbiol. 12, 2450–2465.
Offre, P., Kerou, M., Spang, A., Schleper, C., 2014. Variability of the transporter gene complement in ammonia-oxidizing archaea. Trends Microbiol. 22 (12), 665–675.
Oschlies, A., Brandt, P., Stramma, L., Schmidtko, S., 2018. Drivers and mechanisms of ocean deoxygenation. Nat. Geosci. 11 (7), 467–473.
Osterholz, H., Dittmar, T., Niggemann, J., 2014. Molecular evidence for rapid dissolved organic matter turnover in Arctic fjords. Mar. Chem. 160, 1–10.

Overbeek, R., Begley, T., Butler, R.M., Choudhuri, J.V., Chuang, H.-Y., Cohoon, M., de Crécy-Lagard, V., Diaz, N., Disz, T., Edwards, R., Fonstein, M., Frank, E.D., Gerdes, S., Glass, E.M., Goesmann, A., Hanson, A., Iwata-Reuyl, D., Jensen, R., Jamshidi, N., Krause, L., Kubal, M., Larsen, N., Linke, B., McHardy, A.C., Meyer, F., Neuweger, H., Olsen, G., Olson, R., Osterman, A., Portnoy, V., Pusch, G.D., Rodionov, D.A., Rückert, C., Steiner, J., Stevens, R., Thiele, I., Vassieva, O., Ye, Y., Zagnitko, O., Vonstein, V., 2005. The subsystems approach to genome annotation and its use in the project to annotate 1000 genomes. Nucleic Acids Res. 33, 5691–5702.

Pai, S.-C., Tsau, Y.-J., Yang, T.-I., 2001. pH and buffering capacity problems involved in the determination of ammonia in saline water using the indophenol blue spectrophotometric method. Anal. Chim. Acta 434 (2), 209–216.

Park, B.H., Karpinets, T.V., Syed, M.H., Leuze, M.R., Uberbacher, E.C., 2010. CAZymes Analysis Toolkit (CAT): Web service for searching and analyzing carbohydrate-active enzymes in a newly sequenced organism using CAZy database. Glycobiology 20, 1574–1584.

Parsonage, D., Karplus, P.A., Poole, L.B., 2008. Substrate specificity and redox potential of AhpC, a bacterial peroxiredoxin. PNAS 105 (24), 8209–8214.

Petasne, R.G., Zika, R.G., 1987. Fate of superoxide in coastal sea water. Nature 325 (6104), 516–518.

Plominsky, A.M., Trefault, N., Podell, S., Blanton, J.M., De la Iglesia, R., Allen, E.E., von Dassow, P., Ulloa, O., 2018. Metabolic potential and *in situ* transcriptomic profiles of previously uncharacterized key microbial groups involved in coupled carbon, nitrogen and sulfur cycling in anoxic marine zones. Environ. Microbiol. 20 (8), 2727–2742.

Qian, W., Gan, J., Liu, J., He, B., Lu, Z., Guo, X., Wang, D., Guo, L., Huang, T., Dai, M., 2018. Current status of emerging hypoxia in a eutrophic estuary: The lower reach of the Pearl River Estuary, China. Estuar. Coast. Shelf Sci. 205, 58–67.

Qin, W., Amin, S.A., Martens-Habbena, W., Walker, C.B., Urakawa, H., Devol, A.H., Ingalls, A.E., Moffett, J.W., Armbrust, E.V., Stahl, D.A., 2014. Marine ammonia-oxidizing archaeal isolates display obligate mixotrophy and wide ecotypic variation. PNAS 111 (34), 12504–12509.

Qin, W., Heal, K.R., Ramdasi, R., Kobelt, J.N., Martens-Habbena, W., Bertagnolli, A.D., Amin, S.A., Walker, C.B., Urakawa, H., Könneke, M., 2017. *Nitrosopumilus maritimus* gen. nov., sp. nov., *Nitrosopumilus cobalaminigenes* sp. nov., *Nitrosopumilus oxyclinae* sp. nov., and *Nitrosopumilus ureiphilus* sp. nov., four marine ammonia-oxidizing archaea of the phylum *Thaumarchaeota*. Int. J. System. Evol. Microbiol. 67, 5067–5079.

Qin, W., Zheng, Y., Zhao, F., Wang, Y., Urakawa, H., Martens-Habbena, W., Liu, H., Huang, X., Zhang, X., Nakagawa, T., Mende, D.R., Bollmann, A., Wang, B., Zhang, Y., Amin, S.A., Nielsen, J.L., Mori, K., Takahashi, R., Virginia Armbrust, E., Winkler, M.-K.-H., DeLong, E.F., Li, M., Lee, P.-H., Zhou, J., Zhang, C., Zhang, T., Stahl, D.A., Ingalls, A.E., 2020. Alternative strategies of nutrient acquisition and energy conservation map to the biogeography of marine ammonia-oxidizing archaea. ISME J. 14 (10), 2595–2609.

Robinson, C., 2019. Microbial respiration, the engine of ocean deoxygenation. Front. Mar. Sci. 5, 533.

Saier, M.H., Yen, M.R., Noto, K., Tamang, D.G., Elkan, C., 2009. The transporter classification database: Recent advances. Nucleic Acids Res. 37 (Database), D274–D278.

Sauder, L.A., Ross, A.A., Neufeld, J.D., Bothe, H., 2016. Nitric oxide scavengers differentially inhibit ammonia oxidation in ammonia-oxidizing archaea and bacteria. FEMS Microbiol. Lett. 363 (7), fnw052. https://doi.org/10.1093/femsle/fnw052.

Schleper, C., Nicol, G.W., 2010. Ammonia-oxidising archaea–physiology, ecology and evolution. Adv. Microb. Physiol. 57, 1–41.

Schmidtko, S., Stramma, L., Visbeck, M., 2017. Decline in global oceanic oxygen content during the past five decades. Nature 542 (7641), 335–339.

Schulz, M.H., Zerbino, D.R., Vingron, M., Birney, E., 2012. Oases: robust *de novo* RNA-seq assembly across the dynamic range of expression levels. Bioinformatics 28, 1086–1092.

Shen, T., Stieglmeier, M., Dai, J., Urich, T., Schleper, C., 2013. Responses of the terrestrial ammonia-oxidizing archaeon *Ca. Nitrososphaera viennensis* and the ammonia-oxidizing bacterium *Nitrosospira multiformisto* nitrification inhibitors. FEMS Microbiol. Lett. 344 (2), 121–129.

Song, N.a., Jiang, H.-L., 2020. Coordinated photodegradation and biodegradation of organic matter from macrophyte litter in shallow lake water: Dual role of solar irradiation. Water Res. 172, 115516. https://doi.org/10.1016/j.watres.2020.115516.

Spietz, R.L., Williams, C.M., Rocap, G., Horner-Devine, M.C., 2015. A dissolved oxygen threshold for shifts in bacterial community structure in a seasonally hypoxic estuary. PLoS ONE 10, e0135731.

Stewart, F.J., Ulloa, O., DeLong, E.F., 2012. Microbial metatranscriptomics in a permanent marine oxygen minimum zone. Environ. Microbiol. 14, 23–40.

Suter, E.A., Pachiadaki, M.G., Montes, E., Edgcomb, V.P., Taylor, G.T., 2020. Diverse nitrogen cycling pathways across a marine oxygen gradient indicate nitrogen loss coupled to chemoautotrophic activity. Environ. Microbiol. 23 (6), 2747–2764. https://doi.org/10.1111/1462-2920.15187.

Sutherland, K.M., Coe, A., Gast, R.J., Plummer, S., Suffridge, C.P., Diaz, J.M., Bowman, J. S., Wankel, S.D., Hansel, C.M., 2019. Extracellular superoxide production by key microbes in the global ocean. Limnol. Oceanogr. 64 (6), 2679–2693.

Sutherland, K.M., Wankel, S.D., Hansel, C.M., 2020. Dark biological superoxide production as a significant flux and sink of marine dissolved oxygen. PNAS 117 (7), 3433–3439.

Tang, K., Lin, Y., Han, Y., Jiao, N., 2017. Characterization of potential polysaccharide utilization systems in the marine bacteroidetes *Gramella flava* JLT2011 using a multi-omics approach. Front. Microbiol. 8, 220.

Teeling, H., Fuchs, B.M., Becher, D., Klockow, C., Gardebrecht, A., Bennke, C.M., Kassabgy, M., Huang, S., Mann, A.J., Waldmann, J., Weber, M., Klindworth, A., Otto, A., Lange, J., Bernhardt, J., Reinsch, C., Hecker, M., Peplies, J., Bockelmann, F. D., Callies, U., Gerdts, G., Wichels, A., Wiltshire, K.H., Glockner, F.O., Schweder, T., Amann, R., 2012. Substrate-controlled succession of marine bacterioplankton populations induced by a phytoplankton bloom. Science 336 (6081), 608–611.

Tkacz, A., Hortala, M., Poole, P.S., 2018. Absolute quantitation of microbiota abundance in environmental samples. Microbiome 6, 110.

Tolar, B.B., Powers, L.C., Miller, W.L., Wallsgrove, N.J., Popp, B.N., Hollibaugh, J.T., 2016. Ammonia oxidation in the ocean can be inhibited by nanomolar concentrations of hydrogen peroxide. Front. Mar. Sci. 3, 237.

Ulloa, O., Canfield, D.E., DeLong, E.F., Letelier, R.M., Stewart, F.J., 2012. Microbial oceanography of anoxic oxygen minimum zones. PNAS 109 (40), 15996–16003.

UniProt, C., 2015. UniProt: a hub for protein information. Nucleic Acids Res. 43, D204–D212.

Vaquer-Sunyer, R., Duarte, C.M., 2008. Thresholds of hypoxia for marine biodiversity. PNAS 105 (40), 15452–15457.

Walker, C.B., de la Torre, J.R., Klotz, M.G., Urakawa, H., Pinel, N., Arp, D.J., Brochier-Armanet, C., Chain, P.S.G., Chan, P.P., Gollabgir, A., Hemp, J., Hugler, M., Karr, E. A., Konneke, M., Shin, M., Lawton, T.J., Lowe, T., Martens-Habbena, W., Sayavedra-Soto, L.A., Lang, D., Sievert, S.M., Rosenzweig, A.C., Manning, G., Stahl, D.A., 2010. *Nitrosopumilus maritimus* genome reveals unique mechanisms for nitrification and autotrophy in globally distributed marine crenarchaea. PNAS 107 (19), 8818–8823.

Walters, W., Humphrey, G., Hyde, E.R., Parada, A., Caporaso, J.G., Berg-Lyons, D., Fuhrman, J.A., Gilbert, J.A., Apprill, A., Ackermann, G., Jansson, J.K., Knight, R., 2015. Improved bacterial 16S rRNA gene (V4 and V4–5) and fungal internal transcribed spacer marker gene primers for microbial community surveys. mSystems 1, e00009–e00015.

Winkler, F.K., 2006. Amt/MEP/Rh proteins conduct ammonia. Pflügers Archiv: Eur. J. Physiol. 451 (6), 701–707.

Wright, J.J., Konwar, K.M., Hallam, S.J., 2012. Microbial ecology of expanding oxygen minimum zones. Nat. Rev. Microbiol. 10 (6), 381–394.

Ye, Q.i., Wu, Y., Zhu, Z., Wang, X., Li, Z., Zhang, J., 2016. Bacterial diversity in the surface sediments of the hypoxic zone near the Changjiang Estuary and in the East China Sea. Microbiologyopen 5 (2), 323–339.

Zapata, M., Rodríguez, F., Garrido, J.L., 2000. Separation of chlorophylls and carotenoids from marine phytoplankton: a new HPLC method using a reversed phase C8 column and pyridine-containing mobile phases. Mar. Ecol. Prog. Ser. 195, 29–45.

Zhai, W.-D., Zhao, H.-d., Su, J.-L., Liu, P.-F., Li, Y.-W., Zheng, N., 2019. Emergence of summertime hypoxia and concurrent carbonate mineral suppression in the central Bohai Sea, China. J. Geophys. Res. Biogeosci. 124 (9), 2768–2785.

Zhang, J., Gilbert, D., Gooday, A.J., Levin, L., Naqvi, S.W.A., Middelburg, J.J., Scranton, M., Ekau, W., Peña, A., Dewitte, B., Oguz, T., Monteiro, P.M.S., Urban, E., Rabalais, N.N., Ittekkot, V., Kemp, W.M., Ulloa, O., Elmgren, R., Escobar-Briones, E., Van der Plas, A.K., 2010. Natural and human-induced hypoxia and consequences for coastal areas: Synthesis and future development. Biogeosciences 7 (5), 1443–1467.

Zinser, E.R., 2018a. The microbial contribution to reactive oxygen species dynamics in marine ecosystems. Environ. Microbiol. Rep. 10 (4), 412–427.

Zinser, E.R., 2018b. Cross-protection from hydrogen peroxide by helper microbes: the impacts on the cyanobacterium *Prochlorococcus* and other beneficiaries in marine communities. Environ. Microbiol. Rep. 10 (4), 399–411.